Eighth Australasian Fluid Mechanics
Conference, University of Newcastle,
N.S.W., 28 November/2 December 1983.

COMPUTATIONAL INVESTIGATION OF TURBULENT TRAILING EDGE FLOWS

K. SRINIVAS AND C.A.J. FLETCHER

DEPARTMENT OF MECHANICAL ENGINEERING

UNIVERSITY OF SYDNEY, SYDNEY, N.S.W. 2006 AUSTRALIA

SUMMARY The paper reports the computational investigation of flow in the near-wake region of a trailing edge using a time-split finite element method. Steady-state solutions to the compressible Navier-Stokes equations are sought by solving an equivalent unsteady problem. A Galerkin finite element method with a group formulation is employed and the resulting equations are solved by a three-level implicit algorithm. Computations are performed in a transformed plane and a time-split method for the Navier-Stokes equations in generalised coordinates is developed for the purpose. Further, an algebraic eddy viscosity model is used to represent the Reynolds stresses. Both symmetric and asymmetric trailing edges are considered. Results are presented in the form of velocity profiles and displacement thickness distributions.

1 INTRODUCTION

The flow at the trailing edge of an aerofoil is a challenge to the computational fluid dynamicist because of its complexity. At the same time, the flow is of considerable importance as it plays a major role in aerofoil and turbine blade design. Viscous-inviscid interaction, stream-wise adverse pressure gradients, large pressure gradients normal to the surface and possible separation of flow at the trailing edge are some of the features which make the flow behaviour difficult to predict.

There have been a number of attempts to compute the turbulent flow past a trailing edge. A major contributor is Horstman (1983) who employs MacCormack's time-split method to solve the Navier-Stokes equations with a wedge geometry to simulate the local trailing-edge behaviour. Diewert (1979) computes the flow around a complete aerofoil using MacCormack's explicit-implicit-characteristics method and different models of turbulence. Baker et al (1982) have used finite-element method to compute turbulent flow over a complete aerofoil. The methods employed seem to be capable, in general, of predicting many features of the flow. Most of the previous studies have relied on differential equation models of turbulence like the k-ε or the k-ω^2 model. Usually, it is held that algebraic models of turbulence are not adequate for predicting accurately the trailing-edge flows. We examine this claim further in this paper.

Here, we consider turbulent flows past a symmetric and an asymmetric trailing edge; the geometry of the latter is similar to that used by Horstman (1983). This work is a continuation of our computational studies of turbulent flows.

Previously (Srinivas and Fletcher, 1983), the flow past a flat plate and a backward-facing step has been computed using ADIFEM, an alternating direction implicit finite element method (Fletcher, 1982). Mean-flow features such as velocity profiles, reattachment length, pressure distribution were obtained in good agreement with experimental data. An (algebraic) eddy viscosity model was used to represent the Reynolds stresses. The investigation indicated that a simple algebraic model was adequate to predict the mean flow except in the region downstream of reattachment. However more elaborate two-equation turbulence models are also inaccurate in this region (Horstman, 1977).

The geometry of the trailing edge requires a distorted mesh close to it and calls for the use of special procedures like the isoparametric formulation. Here we follow the more efficient route of expressing the governing equations in generalised coordinates (ξ,η). A time-split finite-element method, employed as the computational algorithm, is a further development of ADIFEM. We use a three-level scheme in place of the two-level scheme and only evaluate the steady-state residual once per time-step. Further, a consistent time-splitting is achieved in the present work by extracting mass and difference operators (Fletcher and Srinivas, 1983).

The time-split finite element method and the eddy viscosity model used to represent the Reynolds stresses are described briefly in Section 2. In Section 3 mean velocity profiles and displacement thickness profiles are presented and discussed for the flow past symmetric and asymmetric trailing-edges.

2 TIME-SPLIT FINITE ELEMENT METHOD

The flow is governed by the unsteady, two-dimensional, Navier-Stokes equations. Here the unsteady equations provide an appropriate iterative framework to reach a steady-state solution; time plays the role of an iteration parameter. The equations in Cartesian co-ordinates are given by Srinivas and Fletcher (1983) and are not repeated here. The temperature changes in the solution domain are expected to be small, an assumption justified for transonic flows. Hence, the molecular viscosity is assumed to be constant everywhere. The following equation is used to calculate pressure thus eliminating the energy equation from consideration.

$$p = \rho\left\{RT_o - \frac{\gamma-1}{2\gamma}(u^2 + v^2)\right\} \qquad (1)$$

Now, under a general transformation

$$\xi = \xi(x,y),\ \eta = \eta(x,y) \qquad (2)$$

the governing equations become

$$\bar{q}_t + \bar{F}_\xi + \bar{G}_\eta - \bar{R}_{\xi\xi} - \bar{S}_{\xi\eta} - \bar{T}_{\eta\eta} = 0 \qquad (3)$$

Each of the terms q, F, G, R, S and T has three components, one each from the continuity, x-momentum and Y-momentum equations. For example, the components of $\bar{q}$ are $\frac{\rho}{J}$, $\frac{\rho u}{J}$, $\frac{\rho v}{J}$. J is the Jacobian of transformation. The other symbols have their usual meanings.(see appendix)

An application of the group Galerkin finite-element method (Fletcher, 1983) with linear Lagrange elements gives the following set of ordinary differential equations.

$$M_\xi \otimes M_\eta \, \bar{q}_t + M_\eta \otimes L_\xi \, \bar{F} + M_\xi \otimes L_\eta \, \bar{G} - M_\eta \otimes L_{\xi\xi} \, \bar{R} - L_\xi \otimes L_\eta \, \bar{S} - M_\xi \otimes L_{\eta\eta} \, T = 0 \qquad (4)$$

where M_ξ and M_η are mass operators and L_ξ, L_η, $L_{\xi\xi}$ and $L_{\eta\eta}$ are the difference operators (Fletcher and Srinivas, 1983) and $\otimes$ denotes the tensor product.

Equation (4) is solved by employing the following two-stage, three-level algorithm -

$$\left[M_\xi - \frac{\beta}{\alpha}\Delta t \left(L_{\xi\xi}\frac{\partial \bar{R}}{\partial \bar{q}} - L_\xi \frac{\partial \bar{F}}{\partial \bar{q}}\right)\right] \Delta \bar{q}^* = \frac{\Delta t}{\alpha}(\text{RHS}) - \frac{(1-\alpha)}{\alpha} M_\xi \otimes M_\eta \, \Delta \bar{q}^n$$

$$\left[M_\eta - \frac{\beta}{\alpha}\Delta t \left(L_{\eta\eta}\frac{\partial \bar{T}}{\partial \bar{q}} - L_\eta \frac{\partial \bar{G}}{\partial \bar{q}}\right)\right] \Delta \bar{q}^{n+1} = \Delta \bar{q}^* \qquad (5)$$

where (RHS) $= M_\eta \otimes L_{\xi\xi} \, \bar{R} + L_\xi \otimes L_\eta \, \bar{S} + M_\xi \otimes L_{\eta\eta} \, \bar{T} - M_\eta \otimes L_\xi \, \bar{F} - M_\xi \otimes L_\eta \, \bar{G} + \beta \Delta t \, L_\xi \otimes L_\eta \left(\frac{\partial \bar{S}}{\partial \bar{q}}\right) \Delta \bar{q}.$

A choice of $\alpha = 1.5$ and $\beta = 1.0$ has been used in the present study. A description of the features of the computational algorithm is provided by Fletcher and Srinivas (1983).

2.1 Eddy Viscosity Model

With the wide-spread usage of differential equation models of turbulence, there is a tendency to question the validity of a purely algebraic representation for the eddy viscosity especially for flows as complex as the one at a trailing edge. But our experience with wake flows and the flow over a backward facing step (Srinivas and Fletcher, 1983) is quite encouraging. The only disadvantage of using an algebraic eddy viscosity model is its poor prediction of shear stress following reattachment in the case of flow over a backward-facing step. However, two-equation (differential) models also fail to predict accurately the shear stress following reattachment. Further, they fail to predict correctly the reattachment length (Eaton, 1981). On the other hand, the studies by Deiwert (1979) employing both the algebraic and differential equation models bring out a very useful feature of algebraic eddy viscosity models. Although considerable differences are found in the prediction of the shear stress, the effect of these on the mean velocity profiles is small and on the surface pressure distribution the effect is negligible.

We are mainly interested in the pressure distribution over the surface and displacement thickness. Judging by our previous experience and that of others, algebraic eddy viscosity models seem to be adequate. The model used here is as follows:-

(a) Inner region of the boundary layer

$$\varepsilon = \rho \, k_1^2 \, y^2 \, D^2 \, \left| \, (u_y^2 + v_x^2)^{\frac{1}{2}} \, \right| \qquad (6)$$

(b) Outer region of the boundary layer and wake

$$\varepsilon = k_2 \, \rho \, U_{max} \, \delta^* \, \gamma \qquad (7)$$

The symbols have their usual meanings (Srinivas and Fletcher, 1983).

To take into account the upstream history of turbulence a relaxation is carried out as explained in the above reference.

3. RESULTS AND DISCUSSION

The geometry of the trailing edge considered is given in Fig. 1. The geometry of the symmetric trailing edge is similar to that used by Viswanath, et al (1979) whereas the geometry of the asymmetric trailing edge is similar to that examined by Horstman (1983). The rectangle AGFE in the physical domain is transformed to a rectangle A'G'F'E' in the computational domain while the wedge BCD is transformed to a straight line D'C'. The gradients of u and v velocity components are assumed to vanish on FG where the pressure is calculated by imposing the non-reflecting conditions (Srinivas and Fletcher, 1983). On AG and EF u-velocity and density are held constant at their freestream values while pressure is calculated by imposing the non-reflecting conditions. The imposition of boundary conditions on DE and AB follows the procedure outlined in the above reference. Further, we adopt the law of the wall approach and force the velocity at points on rows adjacent to solid walls. This procedure is also outlined in the same reference.

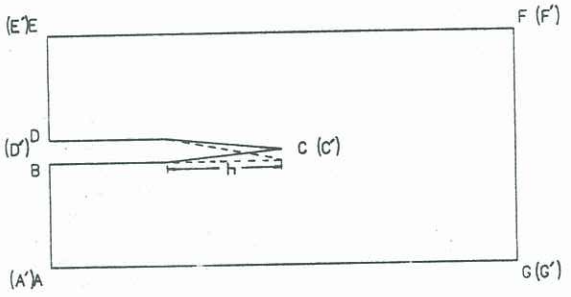

Figure 1 Geometry of the trailing edge considered. (——— symmetric, — — — asymmetric)

Region AGFE was divided into 34x82 linear elements. The mesh spacing was uniform in both the x and y directions in regions close to C. Away from C the mesh was stretched geometrically by a factor of 1.35 in the x-direction and 1.07 in the y-direction. Such a mesh spacing was necessary to achieve a good resolution of the flow behaviour close to the trailing edge, C. The mesh spacing in the ξ and η directions in the computational domain was similar.

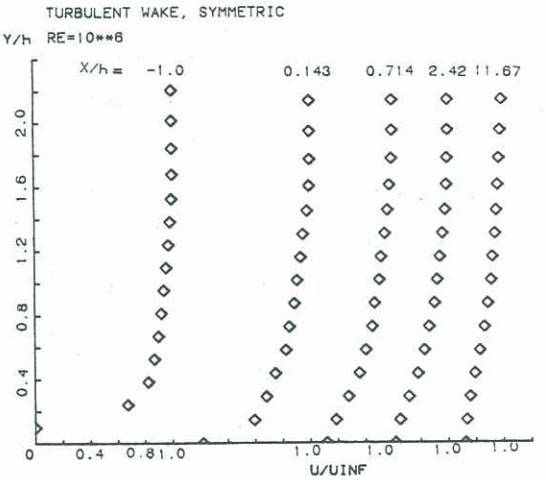

Figure 2 Mean velocity profiles for the symmetric trailing edge (x measured from C, see Fig. 1).

Computations were carried out for a Reynolds number of 10^6 and a freestream Mach number of 0.4. The mean velocity profiles at various x-stations for the symmetric trailing edge are given in Fig. 2. A rapid increase in the x-direction is observed to take place in the mean velocity values closer to the central line in the near wake. Away from the central line the profiles retain their character found upstream of the trailing edge. In the far wake region, however, changes are observed in the profiles away from the central line due to the influence of the trailing edge.

Displacement thickness is a critical parameter which is of use in aerofoil design. Fig. 3 shows a distribution of displacement thickness in the x-direction. Here the displacement thickness has been expressed as a ratio of that at the inlet). It is observed that in the far wake region the displacement thickness recovers to a value equal to that at inlet.

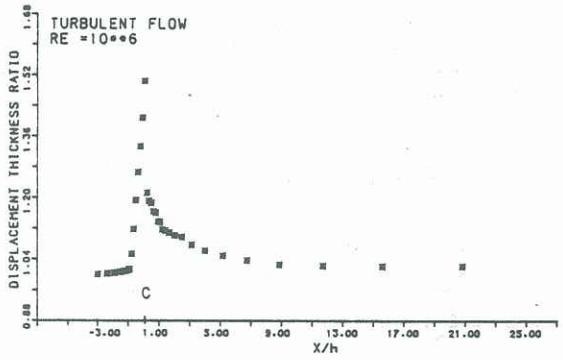

Figure 3 Displacement thickness distribution for the symmetric trailing edge. (X measured from C, see Fig. 1.)

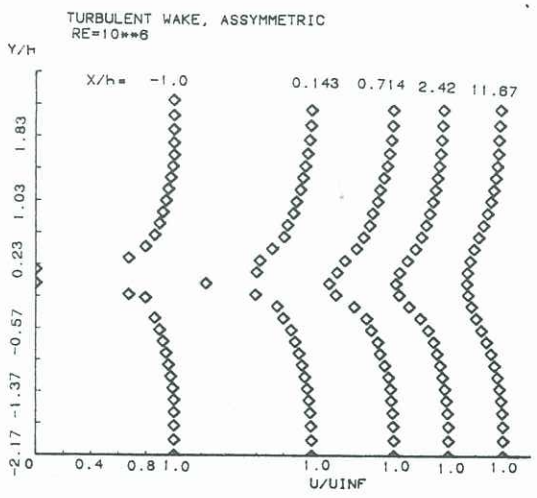

Figure 4 Mean velocity profiles for the asymmetric trailing edge. (X measured from C, see Fig. 1.)

Fig. 4 shows the mean velocity profiles for various x-stations for the asymmetric configuration. The effect of the trailing edge geometry is strongly felt in the near-wake regions close to the central line. As the far-wake region is approached the profiles assume a symmetric character. This is also true of the distribution of displacement thickness shown in Fig. 5. The displacement thickness for the upper surface at the trailing edge C' (see Fig. 1) is seen to be about 2.1 times that at the inlet. Computations of Horstman (1983) for a similar geometry and the same freestream Mach number indicate a rise in displacement thickness by a factor of about 2.5 at the trailing edge when using a k-ε turbulence model.

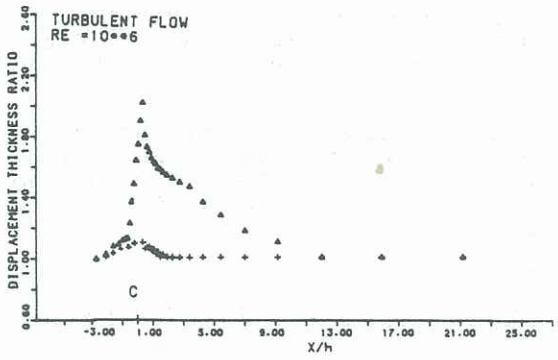

Figure 5 Displacement thickness distribution for the asymmetric trailing edge. (Δ, upper surface, +, lower surface, X measured from C, see Fig. 1.)

The pressure distribution (not shown here) around the asymmetric trailing edge is also found to be in good agreement with that observed by Horstman (1983). We have not attempted a detailed comparison of our results with those of Horstman, here. Such a comparison, including an assessment of the current eddy viscosity model will be made after computing the flow at different Mach numbers.

4 ACKNOWLEDGEMENTS

The authors are grateful to the Australian Research Grants Committee for their continued financial support.

5 REFERENCES

BAKER, A.J., YU, J.C., ORZECHOWSKI, J.A. and GATSKI, T.B. (1982) Prediction and Measurement of Incompressible Turbulent Aerodynamic Trailing Edge Flows. AIAA J., 20, pp. 51-59.

DEIWERT, G.S. (1979) Computation of Turbulent Near Wake for Asymmetric Airfoils. NASA TM 78581.

FLETCHER, C.A.J. (1982) On an Alternating Direction Implicit Finite Element Method for Flow Problems. Comp. Meth. Appl. Mech. Eng., 30, pp. 307-322.

FLETCHER, C.A.J. (1983) The Group Finite Element Formulation. Comp. Meth. Appl. Mech. Engn., 37, pp. 225-243.

FLETCHER, C.A.J. and SRINIVAS, K. (1983) Stream Function Vorticity Revisited. Comp. Meth. Appl. Mech. Engn. (submitted).

EATON, J.K. (1981) Summary of Computations for Case 0421 - Backward-facing Step Flow. 1980-81 AFOSR-HTTM-Stanford Conference on Complex Turbulent Flows.

HORSTMAN, C.C., SETTLES, G.S., VAS, I.E., BOGDONOFF, S.M. and HUNG, C.M. (1977) Reynolds Number Effects on Shock Wave Boundary-Layer Interactions. AIAA J., 15, pp. 1152-1158.

HORSTMAN, C.C. (1983) Numerical Simulation of Turbulent Trailing Edge Flows. Second Symposium on Numerical and Physical Aspects of Aerodynamic Flows, Long Beach, CA, U.S.A.

SRINIVAS, K. and FLETCHER, C.A.J. (1983) Finite Element Solutions for Laminar and Turbulent Compressible Flow. Int. J. Num. Methods for Fluid Flows (to appear).

VISWANATH, P.R., CLEARY, J.W., SEEGMILLER, H.L., and HORSTMAN, C.C. (1979) Trailing-Edge Flows at High Reynolds Number, AIAA paper 79-1503, 12th Fluid and Plasma Dynamics Conference, July 23-25.

APPENDIX

In equation (3) the terms, $\bar{q}$, $\bar{F}$, $\bar{R}$, $\bar{S}$, and $\bar{T}$ are as follows.

$$\bar{q} = \left\{ \frac{\rho}{J} , \frac{\rho u}{J} , \frac{\rho v}{J} \right\}$$

$$\bar{F} = \frac{1}{J} \begin{Bmatrix} \rho U_c \\ \xi_x p + \rho u U_c + \left(\frac{4\mu'}{3}\xi_{xx} + \mu'\xi_{yy}\right)u + \left(\frac{\mu'}{3}\xi_{xy}\right)v \\ \xi_y p + \rho v U_c + \left(\mu'\xi_{xx} + \frac{4\mu'}{3}\xi_{yy}\right)v + \left(\frac{\mu'}{3}\xi_{xy}\right)v \end{Bmatrix}$$

$$\bar{G} = \frac{1}{J} \begin{Bmatrix} \rho V_c \\ \eta_x p + \rho u V_c + \left(\frac{4\mu'}{3}\eta_{xx} + \mu'\eta_{yy}\right)u + \left(\frac{\mu'}{3}\eta_{xy}\right)v \\ \eta_y p + \rho v V_c + \left(\mu'\eta_{xx} + \frac{4\mu'}{3}\eta_{yy}\right)v + \left(\frac{\mu'}{3}\eta_{xy}\right)u \end{Bmatrix}$$

$$\bar{R} = \frac{1}{J} \begin{Bmatrix} \rho \\ \left(\frac{4\mu'}{3}\xi_x^2 + \mu'\xi_y^2\right)u + \frac{\mu'}{3}\xi_x\xi_y v \\ \left(\mu'\xi_x^2 + \frac{4}{3}\mu'\xi_y^2\right)v + \frac{\mu'}{3}\xi_x\xi_y u \end{Bmatrix}$$

$$\bar{S} = \frac{1}{J} \begin{Bmatrix} 0 \\ 2\left(\frac{4\mu'}{3}\xi_x\eta_x + \mu'\xi_y\eta_y\right)u + \frac{\mu'}{3}\left(\xi_x\eta_x + \xi_y\eta_x\right)v \\ 2\left(\mu'\xi_x\eta_x + \frac{4\mu'}{3}\xi_y\eta_y\right)v + \frac{\mu'}{3}\left(\xi_y\eta_x + \eta_y\xi_x\right)u \end{Bmatrix}$$

$$\bar{T} = \frac{1}{J} \begin{Bmatrix} \rho \\ \left(\frac{4\mu'}{3}\eta_x^2 + \mu'\eta_y^2\right)u + \left(\frac{\mu'}{3}\eta_x\eta_y\right)v \\ \left(\mu'\eta_x^2 + \frac{4}{3}\mu'\eta_y^2\right)v + \left(\frac{\mu'}{3}\eta_x\eta_y\right)u \end{Bmatrix}$$

where $U_c = \xi_x u + \xi_y v$, $V_c = \eta_x u + \eta_y v$

and $\mu' = \mu + \varepsilon$ (μ = molecular viscosity, ε = eddy viscosity).